

# Half-life of the Doubly-magic r-Process Nucleus $^{78}\text{Ni}$

P.T. Hosmer,<sup>1,2</sup> H. Schatz,<sup>1,2,3</sup> A. Aprahamian,<sup>3,4</sup> O. Arndt,<sup>5</sup> R.R.C. Clement\*,<sup>1</sup> A. Estrade,<sup>1,2</sup> K.-L. Kratz,<sup>5,6</sup> S.N. Liddick,<sup>1,7</sup> P.F. Mantica,<sup>1,7</sup> W.F. Mueller,<sup>1</sup> F. Montes,<sup>1,2</sup> A.C. Morton<sup>†</sup>,<sup>1</sup> M. Ouellette,<sup>1,2</sup> E. Pellegrini,<sup>1,2</sup> B. Pfeiffer,<sup>5</sup> P. Reeder,<sup>8</sup> P. Santi<sup>‡</sup>,<sup>1</sup> M. Steiner,<sup>1</sup> A. Stolz,<sup>1</sup> B.E. Tomlin,<sup>1,7</sup> W.B. Walters,<sup>9</sup> and A. Wöhr<sup>4</sup>

<sup>1</sup>National Superconducting Cyclotron Laboratory, Michigan State University, East Lansing, MI 48824, USA

<sup>2</sup>Dept. of Physics and Astronomy, Michigan State University, East Lansing, MI 48824, USA

<sup>3</sup>Joint Institute for Nuclear Astrophysics, Michigan State University, East Lansing, MI 48824, USA

<sup>4</sup>Dept. of Physics, University of Notre Dame, Notre Dame, IN 46556-5670, USA

<sup>5</sup>Institut für Kernchemie, Universität Mainz, Fritz-Strassmann Weg 2, D-55128 Mainz, Germany

<sup>6</sup>HGF Virtuelles Institut für Kernstruktur und Nukleare Astrophysik (<http://www.vistars.de>), Mainz, Germany

<sup>7</sup>Dept. of Chemistry, Michigan State University, East Lansing, MI 48824, USA

<sup>8</sup>Richland, WA 99352, USA

<sup>9</sup>Dept. of Chemistry and Biochemistry, University of Maryland, College Park, MD 20742, USA

(Dated: April 30, 2022)

Nuclei with magic numbers serve as important benchmarks in nuclear theory. In addition, neutron-rich nuclei play an important role in the astrophysical rapid neutron-capture process (r-process).  $^{78}\text{Ni}$  is the only doubly-magic nucleus that is also an important waiting point in the r-process, and serves as a major bottleneck in the synthesis of heavier elements. The half-life of  $^{78}\text{Ni}$  has been experimentally deduced for the first time at the Coupled Cyclotron Facility of the National Superconducting Cyclotron Laboratory at Michigan State University, and was found to be  $110_{-60}^{+100}$  ms. In the same experiment, a first half-life was deduced for  $^{77}\text{Ni}$  of  $128_{-33}^{+27}$  ms, and more precise half-lives were deduced for  $^{75}\text{Ni}$  and  $^{76}\text{Ni}$  of  $344_{-24}^{+20}$  ms and  $238_{-18}^{+15}$  ms respectively.

Doubly-magic nuclei with completely filled proton and neutron shells are of fundamental interest in nuclear physics. The simplified structure of these nuclei and their direct neighbors allows one to benchmark key ingredients in nuclear structure theories such as single-particle energies and effective interactions. Doubly-magic nuclei also serve as cores for shell model calculations, dramatically truncating the model space, thus rendering feasible shell model calculations in heavy nuclei. All this is of particular importance for nuclei far from stability, where doubly-magic nuclei serve as beachheads in the unknown territory of the chart of nuclides [1, 2].

When considering the classic nuclear shell gaps and excluding superheavy nuclei, there are only 10 doubly-magic nuclei, and only four of these are far from stability:  $^{48}\text{Ni}$ ,  $^{78}\text{Ni}$ ,  $^{100}\text{Sn}$ , and  $^{132}\text{Sn}$ . Of these,  $^{48}\text{Ni}$  and  $^{78}\text{Ni}$  are the most exotic ones, and the last ones with experimentally unknown properties.  $^{78}\text{Ni}$  therefore represents a unique stepping stone towards the physics of extremely neutron-rich nuclei. In a pioneering experiment, Engelmann *et al.* [3] were able to identify three  $^{78}\text{Ni}$  events produced by in-flight fission of a uranium beam at the Gesellschaft für Schwerionenforschung (GSI), demon-

strating the existence of this nuclide. We report the first measurement of the half-life of  $^{78}\text{Ni}$  at Michigan State University's National Superconducting Cyclotron Laboratory (NSCL), demonstrating that experiments with  $^{78}\text{Ni}$  are finally feasible. Such a measurement provides a first constraint for nuclear models and can serve as a first indicator of nuclear properties far from stability (See for example [4]).

Very neutron-rich nuclei play an important role in the astrophysical rapid neutron-capture process (r-process) [5, 6]. The r-process is responsible for the origin of about half of the heavy elements beyond iron in nature, yet its site and exact mechanism are still unknown.  $^{78}\text{Ni}$  is the only doubly-magic nucleus that represents an important waiting point in the path of the r-process, where the reaction sequence halts to wait for the decay of the nucleus [7].

One popular astrophysical site for the r-process is the neutrino driven wind off a hot, newborn neutron star in a core-collapse supernova explosion [8]. In this case the r-process begins around mass number  $A = 90$ , with lighter nuclei being produced as less neutron-rich species in an  $\alpha$ -rich freeze-out. For such a scenario  $^{78}\text{Ni}$  would not be directly relevant. However, the  $\alpha$ -rich freezeout fails to accurately reproduce the observed abundances for nuclei with  $A = 80-90$  [9], and the associated r-process does not produce sufficient amounts of the heaviest r-process nuclei around  $A = 195$  [10].

$^{78}\text{Ni}$  is among the important r-process waiting points in models that try to address these issues. Examples include models that assume nonstandard neutron star masses [11], or that are based on a supernova triggered by

\*Current affiliation: Lawrence Livermore National Laboratory, 7000 East Ave. Livermore, CA 94550, USA

<sup>†</sup>Current affiliation: TRIUMF, 4004 Wesbrook Mall, Vancouver, BC V6T 1R9 Canada

<sup>‡</sup>Current affiliation: Los Alamos National Laboratory, Safeguards Science and Technology Group (N-1), E540, Los Alamos, NM 87544, USA

the collapse of an ONeMg core in an intermediate mass star [12]. In these models the neutron-capture process begins at lighter nuclei and the half-life of  $^{78}\text{Ni}$  becomes a direct input. Together with the other already known waiting points,  $^{79}\text{Cu}$  and  $^{80}\text{Zn}$ , the half-life of  $^{78}\text{Ni}$  sets the r-process timescale through the  $N = 50$  bottleneck towards heavier elements, and also determines the formation and shape of the associated  $A = 80$  abundance peak in the observed r-process element abundances. The  $A = 80$  mass region has recently gained importance in light of new observations of the element abundances produced by single (or very few) r-process events as preserved in the spectra of old, very metal-poor stars in the Galactic halo. These observations point to the possibility of two different r-processes [13, 14] being responsible for the origin of light r-process nuclei below  $A < 130$ . Only with accurate nuclear data, especially around  $^{78}\text{Ni} - ^{80}\text{Zn}$ , will it be possible to disentangle the various contributions from neutron-capture processes in different astrophysical sites, and to interpret the data on neutron-capture elements expected from the many new metal-poor stars to be identified in ongoing surveys [15].

In this experiment a secondary beam comprised of a mix of several neutron-rich nuclei around  $^{78}\text{Ni}$  was produced by fragmentation of a 140 MeV/nucleon  $^{86}\text{Kr}^{34+}$  primary beam on a 376 mg/cm<sup>2</sup> Be target at the NSCL Coupled Cyclotron Facility. The average primary beam intensity was 15 pA. Fragments were separated by the A1900 fragment separator [16] operating with full momentum acceptance. A position sensitive plastic scintillator at the dispersive intermediate focus was used to determine the momentum of each beam particle at typical rates of  $10^5$ /s. A 100.9 mg/cm<sup>2</sup> achromatic Al degrader was also placed at the intermediate focus of the separator to provide increased separation.

Each nucleus in the secondary beam was individually identified in-flight by measuring energy loss and time of flight, together with the A1900 momentum measurement. The time of flight was measured between two scintillators separated by about 40 m: one located at the intermediate image of the A1900 and the other located inside the experimental vault. The beam was stopped in a stack of Si detectors of the NSCL Beta Counting System (BCS) [17]. Energy loss was measured in the first two Si detectors, which were separated by a passive Al degrader of variable thickness. The degrader thickness was adjusted to stop the nuclei in a 985  $\mu\text{m}$  double-sided Si strip detector (DSSD). The DSSD was segmented into 40 1 mm strips horizontally on one side, and vertically on the other, resulting in 1600 pixels. The beam was continuously implanted into the DSSD, which registered the time and position of each ion. The typical total implantation rate for the entire detector was under 0.1 per second.

Using the dual-gain capability of the BCS electronics, the DSSD also registered the time and position of any

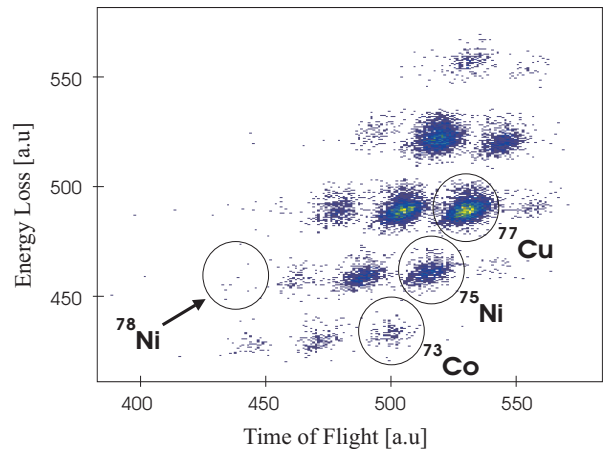


FIG. 1: Particle identification using energy loss vs. time of flight for a subset of the data.

$\beta$ -decays following the implantation of a nucleus. This allowed the correlation of a decay event with a previously identified implanted nucleus. Additional Si detectors in front and behind the DSSD were used to veto events from light particles in the secondary beam that can be similar to  $\beta$ -decay events. With this setup, the total  $\beta$ -type event background rate associated with an implanted ion was typically less than  $3 \times 10^{-2}$ /s. Fig. 1 shows the particle identification using energy loss vs. time of flight. A total of 11  $^{78}\text{Ni}$  events were identified over a total beam time of 104 hours. Using a rough estimate for the integrated beam current and a transmission for  $^{78}\text{Ni}$  fragments into the experimental vault of 65% calculated with the Monte-Carlo beam transport code MOCADI [18], we obtain a rough estimate of the production cross section of  $0.02 \pm 0.01$  pb. This is lower than the estimated cross section from the EPAX formula of 4 pb [19].

Decay half-lives were determined using a maximum likelihood analysis, which has been used before in experiments with low statistics [20], and in extreme cases with just 6 and 7  $\beta$ -decay events [21]. For this work, the formalism was modified to account for  $\beta$ -delayed neutron emission. The method finds the decay constant that maximizes a likelihood function, which is the product of probability densities for three decay generations as well as background events, to produce the measured time sequence of decay-type events following the implantation of a beam particle. The calculation requires knowledge of the  $\beta$ -detection efficiency, background rate, daughter and granddaughter half-lives, including those reached by  $\beta$ -delayed neutron emission, and branchings for  $\beta$ -delayed neutron emission ( $P_n$ ) for all relevant nuclei in the decay chain.

For  $^{75}\text{Ni}$ ,  $^{76}\text{Ni}$ ,  $^{77}\text{Cu}$  and  $^{78}\text{Cu}$  the statistics were sufficient to determine the  $\beta$ -detection efficiency by comparing fitted decay curves with the total number of im-

planted species of that isotope. The resulting efficiencies agree very well and range from 40% to 43% with no systematic trends in the deviation. For  $^{77}\text{Ni}$  and  $^{78}\text{Ni}$ , an average efficiency of  $(42 \pm 1)\%$  was adopted. The background was determined for each run (typical duration of 1h) and in each detector pixel by counting all decay events that occur outside of a 100 s time window following an implantation. Because of the low implantation rate the background is constant over the 5 s time window used to correlate decays to an implantation. Experimental  $P_n$  values as well as daughter and grand-daughter half-lives used for the analysis were taken from [22] and [23] when available. The experimentally unknown  $P_n$  values for the Ni isotopes were taken from detailed spherical quasi-particle random-phase (QRPA) calculations for pure Gamow-Teller (GT) and GT with first-forbidden decay [24] and a number of different choices of single-particle potentials and mass model predictions. From this study, we derive an average uncertainty for the calculated  $P_n$  values of about a factor of two.

The statistical error of the derived decay half-lives is obtained directly from the maximum likelihood analysis. As sources of systematic errors we considered uncertainties in the  $P_n$  values and daughter or grand-daughter half-lives, as well as uncertainties in background rate and detection efficiencies. The systematic uncertainties for the half-lives of  $^{78}\text{Ni}$ ,  $^{77}\text{Ni}$ ,  $^{76}\text{Ni}$ ,  $^{75}\text{Ni}$  are, (in ms)  $^{+33}_{-10}$ ,  $^{+11}_{-7}$ ,  $^{+6}_{-5}$ ,  $^{+8}_{-6}$ , respectively. The main contribution to the systematic errors are uncertainties in the detector efficiency, and uncertainties in the parent  $P_n$  values. In the case of  $^{78}\text{Ni}$ , we also took into account the possibility that one of the events is misidentified. Given the very low number of events beyond  $^{78}\text{Ni}$  in the particle identification (see Fig. 1) this is a very conservative assumption. For  $^{78}\text{Ni}$  this leads to a systematic error of  $^{+10}_{-0}$  ms.

Systematic and statistical errors are correlated since the shape of the likelihood function depends on the analysis parameters. To add systematic and statistical errors we therefore reran the analysis for all combinations of systematic variations and employed the lower and upper one-sigma limits of the resulting statistical errors as the total error budget.

In principle our analysis depends somewhat on the unknown feeding and decay branchings of the known isomeric states in  $^{76}\text{Cu}$  and  $^{77}\text{Zn}$ , which are part of the decay chains considered here. Assuming decay from the isomeric state with a half-life of 1.27 s for  $^{76}\text{Cu}$  would increase the  $^{76}\text{Ni}$  half-life by no more than 12 ms and the  $^{77}\text{Ni}$  half-life by no more than 5 ms. Assuming population of the 1.05 s isomer for  $^{77}\text{Zn}$  could change the half-life of  $^{77}\text{Ni}$  by -8 ms to +13 ms, and the half-life of  $^{78}\text{Ni}$  by -10 ms to +15 ms depending on the probability for that state to  $\beta$ -decay. These uncertainties are based on extreme assumptions with no obvious central value. We therefore give them separately and do not include them in our systematic error bars.

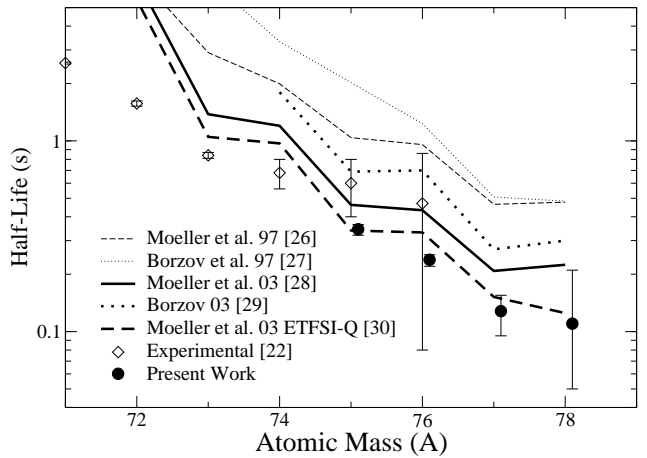


FIG. 2: Experimental Ni half-lives from this and previous work [22] compared to different theoretical calculations.

For the assumption that  $^{76}\text{Cu}$  and  $^{77}\text{Zn}$   $\beta$ -decay from the ground states with half-lives of 0.641 s and 2.08 s respectively [22], our final results are  $344^{+20}_{-24}$  ms for  $^{75}\text{Ni}$ ,  $238^{+15}_{-18}$  ms for  $^{76}\text{Ni}$ ,  $128^{+27}_{-33}$  ms for  $^{77}\text{Ni}$ , and  $110^{+100}_{-60}$  ms for  $^{78}\text{Ni}$ . For  $^{77}\text{Cu}$  and  $^{78}\text{Cu}$ , we obtain  $450^{+13}_{-21}$  ms and  $323^{+11}_{-19}$  ms, in excellent agreement with previous work ( $469 \pm 8$  ms and  $342 \pm 11$  ms) [25].

In Fig. 2 our new experimental half-lives are compared with various theoretical predictions. Often employed in r-process model calculations are the global QRPA calculations of Möller *et al.* 1997 [26] or Borzov *et al.* 1997 [27], the latter being limited to spherical nuclei. Our results show that the trend of these models to over-predict Ni half-lives by factors of 3-4 already observed for the more stable isotopes persists into the path of the r-process at  $^{78}\text{Ni}$ . The recent versions of both models [28, 29] besides other improvements now also include first-forbidden transitions. They clearly lead to better though still somewhat large half-life predictions. Fig. 2 also shows results from calculations with the same model as Möller *et al.* 2003 [28] but using a mass model that includes a quenching of shell gaps far from stability [extended Thomas-Fermi approach + Strutinsky Integral, with shell quenching (ETFSI-Q) [30]]. These calculations give the best agreement with experimental data among the global models.

In order to better understand the nuclear structure in this mass region and to benchmark global models beyond the range of experimental data it is important to test the more sophisticated microscopic calculations, which have been performed for a limited set of singly- and doubly-magic heavy nuclei (see Fig. 3). The self-consistent QRPA approach [31] agrees with the shell-model calculation [32] and the experimental data for most nuclei, but predicts a  $^{78}\text{Ni}$  half-life that even exceeds the experimental  $^{80}\text{Zn}$  half-life. Our measurement clearly fa-

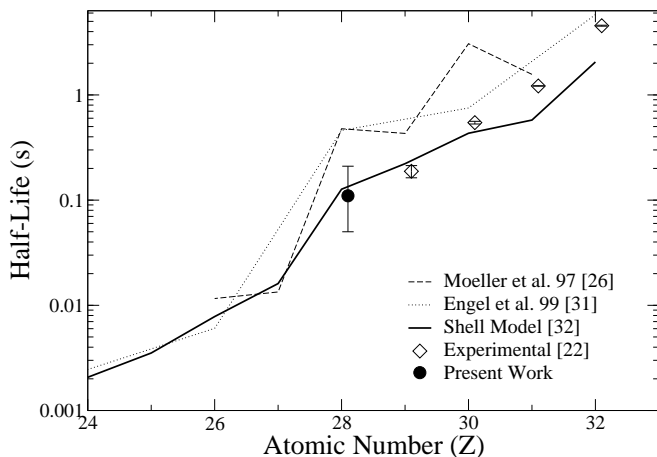


FIG. 3: Theoretical half-life calculations for  $N = 50$  compared to experimental data from this and previous work [22]. Engel *et al.* only gives values for even  $Z$  nuclei.

vors a much lower  $^{78}\text{Ni}$  half-life. On the other hand, the shell model results are in good agreement with experimental data. Of course this does not necessarily mean that the shell-model description of this mass region is entirely correct. For example, deviations in excitation energies, transition strengths, and decay Q-value can in principle compensate each other. More experiments including detailed spectroscopy as they might become possible at future facilities will be needed to clarify this.

In summary, we present the first results for the half-life of  $^{78}\text{Ni}$  and other neutron-rich Ni isotopes. With these results, experimental half-lives are available for all but one ( $^{48}\text{Ni}$ ) classical doubly-magic nuclei. Also, the half-lives of all important  $N = 50$  waiting points in the r-process are now known experimentally. This will make r-process model predictions of the nucleosynthesis around  $A = 80$  more reliable and comparison with observational data more meaningful. It will also put the overall delay that the  $N = 50$  mass region imposes on the r-process flow towards heavier elements on a more solid experimental basis. In this respect the half-life of  $^{78}\text{Ni}$  is of special importance as during the initial stages of the r-process when the heavier nuclei are synthesized the r-process path passes through  $^{78}\text{Ni}$  and  $^{79}\text{Cu}$  rather than through the more stable  $N = 50$  nuclei [33]. The delay timescale for the buildup of heavy elements beyond  $N = 50$  is therefore set by the sum of the lifetimes of  $^{78}\text{Ni}$  and  $^{79}\text{Cu}$ . Our experimental data clearly favor the short timescale of 450 ms obtained with the prediction of Langanke and Martinez-Pinedo [32] over the much longer delays of 960 ms predicted for example by Möller *et al.* [26] leading to an acceleration of the r-process. This is in line with recent improvements in theoretical  $\beta$ -decay half-life predictions along the entire r-process path that also tend to result in shorter half-lives thereby speeding up

the r-process [28]. Detailed r-process model calculations with the new experimental data are beyond the scope of this paper, but will be presented in a forthcoming study.

This work has been supported by NSF grants PHY 01-10253 and PHY 02-16783 (Joint Institute for Nuclear Astrophysics), DFG grant KR 806/13-1, and HGF grant VH-VI-061. H. S. is supported by the Alfred P. Sloan Foundation.

- 
- [1] B. A. Brown, Nucl. Phys. A **704**, 11c (2002).
  - [2] J. Dobaczewski and W. Nazarewicz, Phil. Trans. Math. Phys. Eng. Sci. **356**, 2007 (1998).
  - [3] Ch. Engelmann *et al.*, Z. Phys. A **352** 351 (1995).
  - [4] I. Dillmann *et al.*, Phys. Rev. Lett. **91**, 162503 (2003).
  - [5] F.-K. Thielemann *et al.*, Phys. Rep. **227**, 269 (1993).
  - [6] B. Pfeiffer *et al.*, Nucl. Phys. A **693**, 282 (2001).
  - [7] K.-L. Kratz *et al.*, Ap. J. **403**, 216 (1993).
  - [8] S. E. Woosley and R. D. Hoffman, Ap. J. **395**, 202 (1992).
  - [9] C. Freiburghaus *et al.*, Ap. J. **525**, L121 (1999).
  - [10] K. Takahashi, J. Witti, and H.-T. Janka, Astron. Astrophys. **286**, 857 (1994).
  - [11] T. Terasawa *et al.*, Ap. J. **562**, 470 (2001).
  - [12] S. Wanajo *et al.*, Ap. J. **593**, 968 (2003).
  - [13] B. Pfeiffer *et al.*, "The First Stars". Proceedings of the MPA/ESO Workshop held at Garching, Germany, 4-6 August 1999, edited by A. Weiss, T. G. Abel, and V. Hill (Springer, Berlin, 2000), p.148.
  - [14] C. Travaglio *et al.*, Ap. J. **601**, 864 (2004).
  - [15] T.C. Beers, P. S. Barklem, N. Christlieb and V. Hill, astro-ph/0408381 to be published in Nucl. Phys. A.
  - [16] D.J.Morrissey *et al.*, Nucl. Instrum. Methods B **204**, 90 (2003).
  - [17] J.I.Prisciandaro *et al.*, Nucl. Instrum. Methods A **505**, 140 (2003).
  - [18] N. Iwasa *et al.*, Nucl. Instrum. Methods B **126**, 284 (1997).
  - [19] K. Sümmerer and B. Blank, Phys. Rev. C **61**, 034607 (2000).
  - [20] M.Bernas *et al.*, Z. Phys. A **336** 41 (1990).
  - [21] R.Schneider *et al.*, Nucl. Phys. A **588**, c191 (1995).
  - [22] G. Audi *et al.* Nucl. Phys. A **729**, 3 (2003).
  - [23] B.Pfeiffer *et al.*, Prog. Nucl. Energy **41**, 39 (2002).
  - [24] P. Möller and Randrup, J., Nucl. Phys. A **514**, 1 (1990).
  - [25] K.-L. Kratz *et al.*, Z. Phys. A **340**, 419 (1991).
  - [26] P. Möller, J. R. Nix, and K.-L. Kratz, Atomic Data and Nucl. Data Tab. **66**, 131 (1997).
  - [27] I. N. Borzov, S. Goriely, and J.M. Pearson, Nucl. Phys. A **621**, 307c (1997).
  - [28] P. Möller, B. Pfeiffer, and K.-L. Kratz, Phys. Rev. C **67**, 055802 (2003).
  - [29] I. N. Borzov, Phys. Rev. C **67**, 025802 (2003).
  - [30] J. M. Pearson *et al.* Phys. Lett. B **387**, 455 (1996).
  - [31] J. Engel *et al.* Phys. Rev. C **60**, 014302 (1999).
  - [32] K. Langanke and G. Martinez-Pinedo Rev. Mod. Phys. **75**, 819 (2003).
  - [33] S. Wanajo, r-process movie, at <http://www.ph.sophia.ac.jp/~shinya/research/research.html>